Journal of Materials Chemistry

COMMUNICATION

Field effect transistor based on single crystalline InSb nanowire

Yennai Wang,[a] Junhong Chi,[a] Karan Banerjee,[a] Detlev Grützmacher,[b] Thomas Schäpers[bc] and Jia G. Lu*[a]

InSb nanowires with zinc-blende crystal structure and precise stoichiometry are synthesized *via* pulsed-laser chemical vapor deposition. Raman spectroscopy shows Stokes and anti-Stokes peaks of transverse-optical mode with asymmetric broadening. The nanowire demonstrates n-type semiconductor behavior. Enhanced surface scattering due to size confinement leads to reduced electron mobility.

Semiconductor nanowires have attracted substantial scientific and technological interests due to their unique properties arising from the size confinement effects.[1,2] Group IV, *e.g.* Si, Ge, semiconducting nanowires have been extensively studied. At present, considerable effort has shifted to III–V semiconductors, owing to the advance of band gap engineering and optoelectronics applications.[3] Among the III–V group, indium antimonide (InSb) has the smallest band gap energy (170 meV) at room temperature and possess an extremely high bulk electron mobility.[2,4,5] It has been widely used in infrared opto-electronics and high-speed devices, and has inspired significant interest for fundamental studies in their nanostructure form for potential application as high speed nanoelectronic devices.[6–9] Many groups have reported electrochemical growth of polycrystalline nanowires,[10–13] but only little work has been done on the synthesis and characterizations of single crystalline InSb nanomaterials,[14–17] and a comprehensive transport studies on single nanowire is still lacking. In this paper, we analyze and present how single crystalline InSb nanowires can be synthesized *via* pulse-laser chemical vapor deposition method. The as-obtained nanowires are characterized first by scanning electron microscopy (SEM) and transmission electronic microscopy (TEM), exhibiting highly epitaxial crystalline structure with accurate stoichiometry ratio. Nanowire field-effect transistor (FET) is fabricated on single nanowire by electron beam lithography. It is found that size confinement effect yields a suppressed electron mobility in the InSb nanowires. This effect is also evidenced by the asymmetric broadening of the Raman peaks.

InSb has a low bonding energy of 1.57 eV and has the largest lattice parameter (6.48 Å) of the group III–V semiconductors. The low bond

strength of InSb indicates that it will dissociate easily at high temperatures, thus a low temperature (∼400 °C) is needed for its stable formation. The high lattice parameter of InSb implies that defect-free growth is difficult unless using InSb substrate itself. In order to initiate the vapor liquid solid (VLS) growth of nanowire structure, Au nanoparticles serve as the catalyst medium. From the ternary phase diagram of Au–In–Sb, it follows that the stable phases are $AuIn_2$ and InSb at the synthesis conditions. Stoichiometric InSb growth is also an important issue that needs to be considered due to the low dissociation temperature of InSb as well as the large difference in the melting points of In and Sb. Since the melting point of Sb is higher than the dissociation temperature of InSb, antimony precipitation is favorable during synthesis, resulting in a non-stoichiometry growth. In addition, indium easily vaporizes due to its very low melting point, which further leads to the solid precipitation with an excess amount of antimony than indium. Moreover, the growth environment needs to be extremely pure and completely free of impurities, whose presence can result in the formation of other stable but undesirable phases. This makes the stoichiometric growth of InSb an even challenging task.

To overcome these challenges, the synthesis temperature and the growth substrate play important roles. Three zone CVD growth InSb nanowire has been reported to precisely control the temperatures at InSb source and substrate.[18] In this work, a well-controlled pulsed-laser ablation technique in a single zone chemical vapor deposition (CVD) system is adopted to grow InSb nanowires on an InSb (111) single crystalline substrate (Firebird Technologies).[19,20] The surface oxide of the substrate is first removed by HCl : H_2O and Au nanoparticles are evenly deposited on the substrate as catalysts. The source target of InSb slugs is held in a quartz vial while the growth InSb substrate is placed at the center of the tube furnace. The tube chamber is heated to 470 °C. During the growth process, laser ablation by an Nd : YAG pulsed laser is monitored to precisely stabilized the source plume. Using a laser allows elevating the source to a temperature higher than the dissociation temperature of InSb, while at the same time facilitating the growth substrate to be maintained at a lower temperature than the source. The tube chamber is first evacuated, and then a steady hydrogen flow (5 sccm) is introduced as a carrier gas to maintain the pressure at 200 mtorr. Single crystalline InSb nanowires are then successfully obtained and removed from the substrate after synthesis.

Fig. 1a shows an SEM (Hitachi S-4800) image of the morphology of the freestanding InSb nanowires on the InSb (111) substrate surface. The diameter of the nanowires ranges in 30–50 nm and

[a] Department of Physics & Astronomy and Department of Electrophysics, University of Southern California, Los Angeles, CA, 90089-0484, USA. E-mail: jialu@usc.edu; Fax: +1 21 3740 6653; Tel: +1 21 3821 4328
[b] Institute of Bio- and Nanosystems, Forschungszentrum Jülich GmbH, 52425 Jülich, Germany
[c] JARA-Fundamentals of Future Information Technology, Forschungszentrum Jülich GmbH, 52425 Jülich, Germany
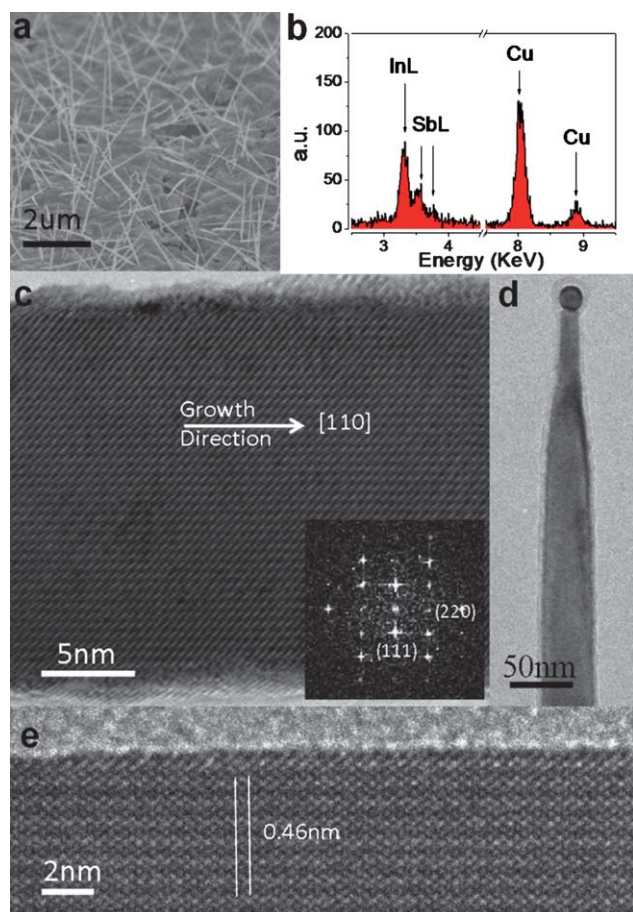
Fig. 1 (a) InSb nanowires grown on single crystalline InSb (111) substrate (scale bar is 2 μm). (b) Single nanowire EDS spectrum shows distinct In, Sb, and Cu peaks. In : Sb ratio is quantified to 1 : 1. (c) TEM image presents nanowire growth direction along [110]. Inset: corresponding FFT displays zinc-blende crystal pattern. (d) Nanowire capped with Au catalyst particle at the tapered tip, manifesting the VLS growth process. (e) HRTEM image shows smooth nanowire surface and clear lattice fringes with a spacing of 0.46 nm corresponding to the (110) plane.

shows a tapered tip at the end; and the length reaches 2–3 micrometres. High resolution TEM (HRTEM) and energy dispersive spectroscopy (EDS) are conducted to further characterize the nanowire material properties. EDS spectrum collected from a single InSb nanowire is demonstrated in Fig. 1b where distinct indium, antimony, and copper peaks are shown. The In : Sb ratio is calculated to be 1 : 1. The Cu peak is contributed from the TEM grid. The HRTEM micrograph displayed in Fig. 1c indicates that the growth direction of nanowire is along [110], where the corresponding inset of Fast Fourier Transform (FFT) plot depicts the pattern of zinc-blende crystal structure of InSb system with 1 : 1 stoichiometric ratio. The tapered single InSb nanowire as shown in Fig. 1d is capped by an Au catalyst particle at the end, thus providing an essential evidence that the growth mechanism of InSb nanowire is governed by VLS process. The enlarged HRTEM image presented in Fig. 1e demonstrates a clean terminated surface of InSb nanowire without any oxide layer formation. In addition, fine lattice fringes demonstrate real space zinc-blende crystal pattern with the inter-plane distance of crystal plane around 0.460 nm. Based on the lattice constant of InSb (0.648 nm),[14] the distance of (110) crystal plane is calculated to be 0.457 nm.

This matches with our observation and confirms that the growth direction of nanowire is along [110] direction.

Raman spectroscopy is performed on a single InSb nanowire. Fig. 2 shows the spectrum collected from Si/SiO₂ substrate with and without the presence of InSb nanowire, and the inset is a SEM image of a single InSb nanowire lying on the substrate. The bottom line represents the background signal purely from Si substrate, and the peaks shown in the top line originate from the InSb nanowire. Both Stokes and anti-Stokes peaks are observed from single nanowire spectrum. Symmetric peaks located at 180 cm⁻¹ and −180 cm⁻¹ are dominant and they correspond to transverse-optical (TO) phonon mode of InSb, as reported for InSb bulk material.[13,21,22] The Stokes peak is more intensive than the anti-Stokes peak, which is typical under thermal equilibrium state.[23,24] In addition, the shoulder peaks emerging at 190 cm⁻¹ and −190 cm⁻¹ correspond to longitudinal-optical (LO) phonon mode. There is no significant Raman shift in the nanowire observed; however, the asymmetric broadening towards the low-frequency side is attributed to the strong phonon confinement effect in InSb nanowire structure.[1,23]

Transport properties are performed by configuring InSb nanowire into a back-gated field-effect transistor (FET). The devices are fabricated *via* conventional electron beam lithography and metallization process onto a single nanowire situated on top of a conducting gate electrode with a 150 nm thick SiO₂ dielectric layer in between. In order to form ohmic contact, the electrodes are made of Cr (20 nm) and Au (60 nm), where Cr has a work function of 4.50 eV close to that of InSb (4.57 eV). Post rapid thermal annealing (RTA) at 250 °C is applied to ensure a good electrical contact. Fig. 3a plots the source–drain current (IDS) *versus* source–drain voltage (VDS) curves at different gate voltages. They exhibit linear behavior suggesting good ohmic contacts, with a resistance around 160 kΩ at zero gate voltage. This corresponds to an upper bound of nanowire resistance due to the 2-probe measurement, and is consistent with the previous report on InSb nanowire grown by CVD method.[15] Gate dependence of source–drain current at different bias voltages is shown in Fig. 3b. The device shows typical n-type semiconductor behaviors, and it is completely turned off below −9 V. The on/off ratio is estimated
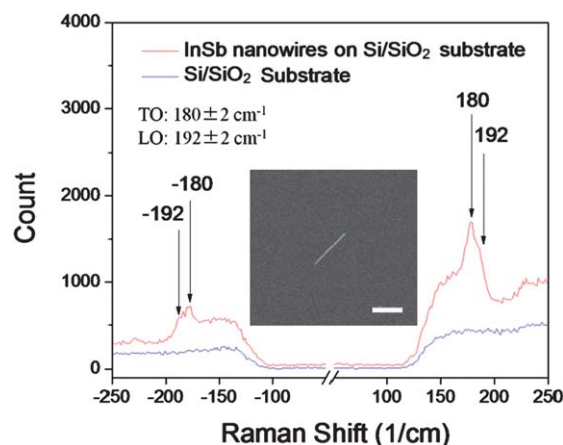

Fig. 2 Raman spectroscopy measurements on a single InSb nanowire on Si/SiO₂ substrate (top line). The bottom line represents the background signal purely from the substrate. Stokes peak (180 cm⁻¹) and anti-Stokes peak (−180 cm⁻¹) are observed and attributed to the TO mode of InSb. Inset: an individual InSb nanowire on the substrate (scale bar is 2 μm) for Raman measurement.
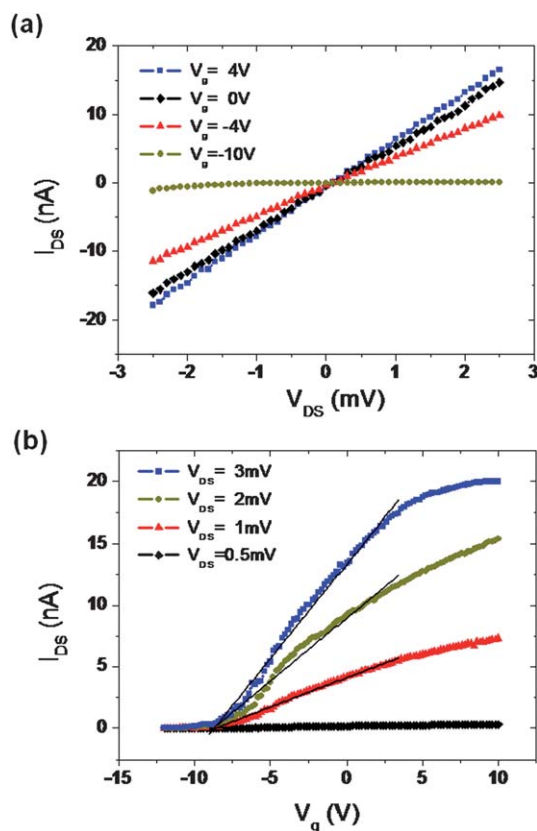
2460 | *J. Mater. Chem.*, 2011, **21**, 2459–2462

This journal is © The Royal Society of Chemistry 2011

Fig. 3 (a) I_{DS} versus V_{DS} of InSb single nanowire FET at different gate voltages. It shows typical n-type semiconductor behaviors with a gate threshold voltage at −9 V. (b) I_{DS} versus V_G at different bias voltages. The threshold voltage is around −9 V while the transconductance dI/dV_G is estimated to be 1.53×10^{-9} A V^{-1}. Carrier concentration ($n = 1.60 \times 10^{18}$ cm^{-3}) and mobility ($\mu_e = 125$ cm^2 V^{-1} s^{-1}) are obtained.

around 10^3 at the drain source voltage $V_{ds} = 3$ mV. The mobility and carrier concentration are estimated for the sample by applying the nanowire field-effect model.[25] With the nanowire diameter of 50 nm and the channel length of 1.37 μm, the electron carrier concentration is estimated to be 1.60×10^{18} cm^{-3}; and the mobility is calculated to be 130 cm^2 V^{-1} s^{-1}, using an effective relative dielectric constant of 2.45 for this back-gate FET device configuration.[26] The mobility is much smaller than the bulk and thin film InSb materials.[4] Similar phenomenon is also observed in other reports.[15,27] Enhanced surface state scattering due to size confinement has dominant effect on the mobility.[2] This is additionally supported by a measurement on another sample with 30 nm wire diameter, showing a reduced mobility of 100 cm^2 V^{-1} s^{-1}. Moreover, the surface scattering at InSb nanowire and Si/SiO$_2$ substrate interface could also contribute to the suppressed mobility. To further elucidate the intrinsic charge transport properties, the temperature variation of electrical conductance will be performed.

In summary, we present the key factors for the synthesis of single crystalline InSb nanowires with precise stoichiometry. The as-grown InSb nanowires possess zinc-blende structure with 1 : 1 In : Sb ratio. High resolution TEM images indicate that the nanowire crystal grows along [110] direction with clean terminated surface. Raman spectroscopy exhibit Stokes and anti-Stokes peaks of InSb transverse-optical phonon, where the asymmetric broadening of peak

intensity originate from the size confinement effect. Field effect transport properties of InSb nanowire devices demonstrate n-type semiconductor characteristics with good gating dependence at small bias voltages. The mobility and carrier concentration obtained from the field effect calculations are estimated to be 125 cm^2 V^{-1} s^{-1} and 1.6 $\times$ 10^{18} cm^{-3}, respectively. The much reduced electron mobility is a result of the enhanced surface scattering due to the size confinement. Much awaits to be explored on the applicability of InSb nanowires as potential nanoscale devices.

Acknowledgements

Notes and references

1 D. L. Chen, C. S. Li, Z. G. Zhu, J. W. Fan and S. Q. Wei, *Phys. Rev. B: Condens. Matter Mater. Phys.*, 2005, **72**, 075341.
2 S. J. Chung, K. J. Goldammer, S. C. Lindstrom, M. B. Johnson and M. B. Santos, *J. Vac. Sci. Technol., B*, 1999, **17**, 1151–1154.
3 R. X. Yan, D. Gargas and P. D. Yang, *Nat. Photonics*, 2009, **3**, 569–576.
4 M. C. Debnath, T. Zhang, C. Roberts, L. F. Cohen and R. A. Stradling, *J. Cryst. Growth*, 2004, **267**, 17–21.
5 J. Riikonen, T. Tuomi, A. Lankinen, J. Sormunen, A. Saynatjoki, L. Knuuttila, H. Lipsanen, P. J. McNally, L. O'Reilly, A. Danilewsky, H. Sipila, S. Vaijarvi, D. Lumb and A. Owens, *J. Mater. Sci.: Mater. Electron.*, 2005, **16**, 449–453.
6 J. H. Seol, A. L. Moore, S. K. Saha, F. Zhou, L. Shi, Q. L. Ye, R. Scheffler, N. Mingo and T. Yamada, *J. Appl. Phys.*, 2007, **101**, 023706.
7 T. Ashley, A. B. Dean, C. T. Elliott, G. J. Pryce, A. D. Johnson and H. Willis, *Appl. Phys. Lett.*, 1995, **66**, 481–483.
8 Y. X. Zhang and F. O. Williamson, *Appl. Opt.*, 1982, **21**, 2036–2040.
9 M. A. Khayer and R. K. Lake, *IEEE Int. Electron Devices Meet., Tech. Dig., 50th*, 2008, 193–196.
10 M. I. Khan, X. Wang, K. N. Bozhilov and C. S. Ozkan, *J. Nanomater.*, 2008, 698759.
11 X. X. Xu, W. Wei, X. M. Qiu, K. H. Yu, R. B. Yu, S. M. Si, G. Q. Xu, W. Huang and B. Peng, *Nanotechnology*, 2006, **17**, 3416–3420.
12 Y. W. Yang, L. Li, X. H. Huang, M. Ye, Y. C. Wu and G. H. Li, *Appl. Phys. A: Mater. Sci. Process.*, 2006, **84**, 7–9.
13 X. R. Zhang, Y. F. Hao, G. W. Meng and L. D. Zhang, *J. Electrochem. Soc.*, 2005, **152**, C664–C668.
14 H. D. Park, S. M. Prokes, M. E. Twigg, Y. Ding and Z. L. Wang, *J. Cryst. Growth*, 2007, **304**, 399–401.
15 R. K. Paul, M. Penchev, J. B. Zhong, M. Ozkan, M. Ghazinejad, X. Y. Jing, E. Yengel and C. S. Ozkan, *Mater. Chem. Phys.*, 2010, **121**, 397–401.
16 D. Candebat, Y. Zhao, C. Sandow, B. Koshel, C. Yang and J. Appenzeller, in *Device Research Conference, 2009*, DRC, 2009, pp. 13–14.
17 Z. Feng, et al., *J. Phys. D: Appl. Phys.*, 2010, **43**, 025406.
18 X. Yang, G. Wang, P. Slattery, J. Z. Zhang and Y. Li, *Cryst. Growth Des.*, 2010, **10**, 2479–2482.
19 C. Jiajun, W. Kai, H. Rong, T. Saito, Y. H. Ikuhara, T. Hirayama and Z. Weilie, *IEEE Trans. Nanotechnol.*, 2010, **9**, 634–639.
20 T. Premkumar, Y. S. Zhou, Y. F. Lu and K. Baskar, *ACS Appl. Mater. Interfaces*, 2010, **2**, 2863–2869.
21 O. Degtyareva, V. V. Struzhkin and R. J. Hemley, *Solid State Commun.*, 2007, **141**, 164–167.
22 T. Nakagawa, K. Ohta and N. Koshizuka, *Jpn. J. Appl. Phys.*, 1980, **19**, L339–L341.
23 T. Horiuchi and N. Wada, *Physics of Semiconductors, Pts A and B*, 2007, **893**, 927–928.

This journal is © The Royal Society of Chemistry 2011

J. Mater. Chem., 2011, **21**, 2459–2462 | 2461

24 V. Wagner, D. Drews, N. Esser, D. R. T. Zahn, J. Geurts and W. Richter, *J. Appl. Phys.*, 1994, **75**, 7330–7333.

25 R. Martel, T. Schmidt, H. R. Shea, T. Hertel and P. Avouris, *Appl. Phys. Lett.*, 1998, **73**, 2447–2449.

26 R. S. Thompson, D. Li, C. M. Witte and J. G. Lu, *Nano Lett.*, 2009, **9**, 3991–3995.

27 S. Vaddiraju, M. K. Sunkara, A. H. Chin, C. Z. Ning and G. R. Dholakia, *J. Phys. Chem. C*, 2007, **111**, 7339–7347.